[35]I. N. Dubrovskaya, Yu. I. Ravich, and O. S. Gryaznov, Fiz. Tekhn. Poluprov. 3, 1770 (1969) [Sov. Phys. Semicond. 3, 1500 (1970)].
[36]K. F. Cuff, M. R. Ellett, C. D. Kuglin, and L. R. Williams, in *Proceedings of the Seventh International Conference on Physics of Semiconductors, Paris*, 1964, edited by M. Hulin (Dunod, Paris, 1964), Vol. I, p. 678.
[37]J. C. McGroddy, in Ref. 6.
[38]C. A. Klein, Phys. Rev. 39, 2029 (1968).
[39]D. J. Olechna and H. Ehrenreich, J. Phys. Chem. Solids 23, 1513 (1962).

PHYSICAL REVIEW B VOLUME 6, NUMBER 6 15 SEPTEMBER 1972

Determination of the Deformation-Potential Constant of the Conduction Band of Silicon from the Piezospectroscopy of Donors*

V. J. Tekippe,† H. R. Chandrasekhar, P. Fisher, and A. K. Ramdas
Department of Physics, Purdue University, Lafayette, Indiana 47907
(Received 1 March 1972)

A piezospectroscopic study of the Lyman spectra of arsenic, antimony, phosphorus, and magnesium donors in silicon has been made using a quantitative-stress cryostat. Within experimental error, all four impurities yield the same value for the shear-deformation-potential constant Ξ_u of the $\langle 100 \rangle$ conduction-band minima. The average value of Ξ_u thus obtained is 8.77 ± 0.07 eV. The shift of the $1s(A_1)$ ground state under stress is characterized by a value of Ξ_u which is lower than the above, viz., 8.3, 8.1, and 7.0 eV for antimony, phosphorus, and arsenic, respectively.

I. INTRODUCTION

Piezospectroscopic studies of the excitation spectra associated with donors and acceptors in semiconductors have proved to be very useful in establishing the site symmetries of the impurities and in providing a symmetry classification of the impurity states.[1] If, in addition, a quantitative stress is employed in such experiments, the deformation-potential constants may be determined for both the ground and excited states. To the extent that these states are described in terms of the band structure,[2] i.e., the conduction-band minima for the donor states and the valence-band maximum for acceptor states in silicon and germanium, these deformation-potential constants should be closely related to the corresponding deformation-potential constants of the band extrema.[3,4] For the donor states, in the effective-mass approximation,[3] these constants should be exactly equal to those of the conduction-band minima, whereas for acceptors they have been shown to be related through numerical factors to those of the valence-band maximum.[4] For silicon, Krag *et al.*[5,6] have reported values for the shear-deformation-potential constant of the conduction-band minima Ξ_u from the piezospectroscopic studies of sulphur, phosphorus, and bismuth donors. These values range from 7.1 to 7.9 eV and differ significantly from the 11-eV value determined by Wilson and Feher[7] and Watkins and Ham[8] using electron-paramagnetic-resonance (EPR) measurements on group-V and lithium donors, respectively. Also, the value for Ξ_u determined by a variety of other techniques lies in the range 8–9 eV (see Table I). We have designed and constructed a quantitative-stress cryostat and have measured Ξ_u from the piezospectroscopic effects of the Lyman spectra of donors in silicon. The present paper reports the results of this investigation.

II. EXPERIMENTAL APPARATUS AND PROCEDURE

The Perkin-Elmer double-pass monochromator (Model No. 112 G) and its associated entrance and exit optics used in these measurements have been described elsewhere.[9] The quantitative-stress cryostat utilized is an adaptation of a glass cryostat used for a number of years in our laboratory (see Fig. 1).[10] The modification consists of replacing the glass centerpiece by one of stainless steel designed to allow an adjustable uniaxial compression to be applied to the sample. The stress centerpiece was also designed to give quantitative information about the stress, very low frictional losses, good cryogenic contact between the sample and the coolant, and a reasonable length of coolant time. In addition, the design parameters allowed for a force in excess of 1×10^8 dyn to be applied to the sample under study.

Figure 2 shows the stress centerpiece; details of the upper and lower sections are shown in Figs. 3 and 4, respectively. The centerpiece is mated to the optical cryostat by means of the stainless-steel cone joint[11] *G*. The pressure head[12] *B* is pressurized with nitrogen gas through the port *A* and the resultant force produced by the piston is transmitted by a hollow push rod *H* which passes through the coolant *I* and makes contact with the

TABLE I. Comparison of values of Ξ_u for silicon determined by various methods.

	Method	Ξ_u(eV)	Ref. No.
1.	Piezospectroscopy of donors (excited states of Sb, P, As, Mg).	8.77±0.07 (~10 °K)	Present work
2.	Piezospectroscopy of the excited states of sulfur donors in silicon.	7.9±0.2 (low temp.)	5
3.	Piezospectroscopy of phosphorus donors in silicon.	7.9±0.2 (10 °K)	6
4.	Piezospectroscopy of the indirect absorption edge.	8.6±0.2 (80 °K), 9.2±0.3 (295 °K)	a
5.	Piezospectroscopy of the indirect exciton spectrum.	8.6±0.4 (77 °K)	b
6.	Linewidth of cyclotron resonance.	8.5±0.1 (2.5–5 °K)	c
7.	Piezoresistance.	8.3±0.3 (77 °K)	d
8.	Piezo-optic effect.	11.3±1.3 (300 °K)	29
9.	Effect of uniaxial stress on EPR of group-V donors.	11±1 (1.25 °K)	7
10.	Effect of uniaxial stress on EPR of lithium donors.	11.4±1.1 (1.3–4 °K)	8
11.	Effect of carrier concentration on elastic constants.	8.6±0.4 (298 °K)	26

[a]I. Balslev, Phys. Rev. 143, 636 (1966).

[b]L. D. Laude, F. H. Pollak, and M. Cardona, Phys. Rev. B 3, 2623 (1971).

[c]R. Ito, H. Kawamura, and M. Fukai, Phys. Letters 13, 26 (1964).

[d]J. E. Aubrey, W. Gubler, T. Henningsen, and S. H. Koenig, Phys. Rev. 130, 1667 (1963).

sample O. The sample is compressed against the bottom of a hollow copper cylinder Q which is threaded to the coolant reservoir J; Q will be referred to as the tail piece in the rest of the description. Two apertures were cut in the lower portion of the tail piece to allow light to pass through the sample. This tail piece is readily interchangeable with others such as one having a third window for right-angle Raman scattering.[13] In such studies, the tail piece was made of stainless steel rather than copper so that stresses of an order of magnitude higher than those employed in the present investigation could be applied. After being transmitted by the sample, the force is returned to the top of the centerpiece via the walls of the reservoir.

The coolant is introduced through the hollow push rod by removing the pressure head. Small holes K and N in the lower section of the push rod allow the coolant to flow into J; note that, as shown in Fig. 4, the lowest portion L of the push rod is made of copper to insure good cryogenic contact. The hole N also serves to remove efficiently any precoolant. With the present design of the stress centerpiece, liquid helium typically lasts about $10\frac{1}{2}$ h with an initial charge of $\sim\frac{3}{4}$ liter.

The lower bellow[14] M completes the vacuum seal between the optical cryostat and the stress centerpiece. The upper bellow D maintains the alignment of the push rod and seals off the space above the coolant forcing the evolved gas through the port F. The rate of evaporation of the liquid coolant can thus be monitored directly by means of a gas-flow-rate meter.[15] In addition, the spring constants of the upper and lower bellows were chosen so that they suspend the push rod in static equilibrium. The height adjustment collar C is used to adjust the equilibrium position of the push rod to be just in contact with the sample at zero gas pressure thus insuring efficient transmission of the applied force from the pressure head to the sample. The adjustable collar E serves as a safety stop in the event of sample breakage.

Nitrogen gas from a commercial cylinder is used to pressurize the pressure head. The pressure is adjusted by means of a regulator[16] and measured by two precision gauges[17] having maximum ranges of 30 and 100 lb/in.^{2}. The pressure head was calibrated initially against a tensile-stress apparatus.[18] Later it was found that calibration against a commercial platform scale[19] was more convenient and accurate for the relatively small pressures used in the present experiments. Figure 5 shows two of the calibration runs using the platform scale. Nonlinear effects at very low pressures and hysteresis effects are avoided by always making measurements above ~5 lb/in.^{2} in the direction of increasing pressure.

The samples cut from suitably doped ingots of silicon were oriented with either x rays or the optical technique of Hancock and Edelman.[20] The optical surfaces were prepared by grinding with carborundum of successively finer grit followed by an etch; during the sample preparation special care was exercised to maintain the desired crystallographic directions. Typical sample dimensions were 20×5×2 mm, the long dimension being the direction of compression. The cross-sectional area was determined by measurements with a depth gauge; this was checked by measuring the length and mass of the sample and calculating the cross section using the known value of the density of silicon.[21] The accuracy of the measurement of the

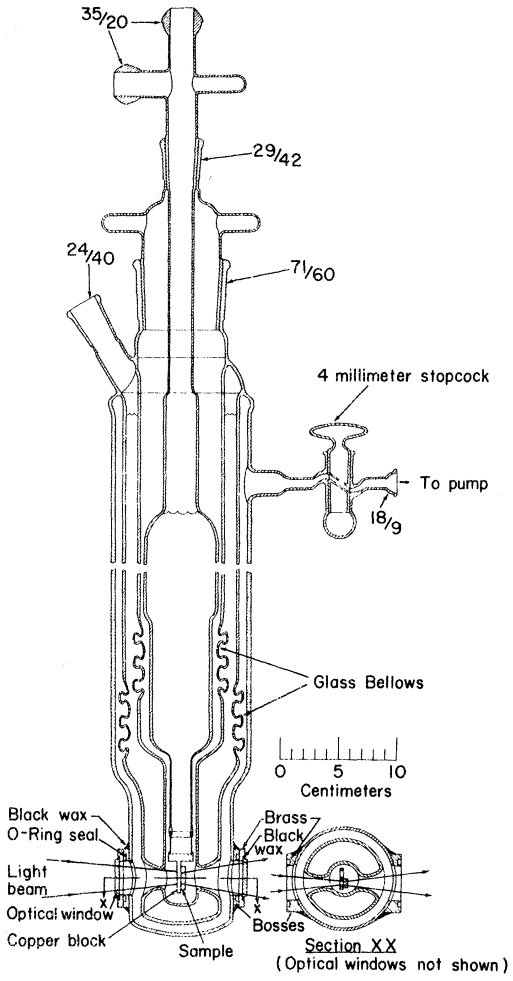

FIG. 1. Glass optical cryostat with glass centerpiece (see Ref. 10).

cross-sectional area is estimated to be about 0.5%. The ends of the sample were ground perpendicular to the length of the sample and glued[22] into the copper cups P shown in Fig. 4. The bottom of the lower cup was coated with a thin layer of Apiezon-N grease to improve the thermal contact with the tail piece.

III. THEORETICAL CONSIDERATIONS

A uniaxial stress applied to a multivalley semiconductor shifts the conduction-band minima with respect to one another. Following Herring's deformation-potential analysis,[23] the shift in energy of the jth minimum, which lies along ⟨100⟩ for Si, is given by

$$\Delta E^{(j)} = \sum_{\alpha,\beta} [\Xi_d \delta_{\alpha\beta} + \Xi_u K_\alpha^{(j)} K_\beta^{(j)}] u_{\alpha\beta} , \qquad (1)$$

where $K_\alpha^{(j)}$ and $K_\beta^{(j)}$ are components of a unit vector pointing from the center of the Brillouin zone towards the position in k space of the jth minimum. The subindex α or β designates a component along one of the cubic axes of the crystal, and $u_{\alpha\beta}$ are the components of the strain tensor. The symbols Ξ_d and Ξ_u are the deformation-potential constants. In the effective-mass theory of donors, the donor wave functions are Bloch functions characterizing the conduction-band minima, modulated by "hydrogenlike" envelope wave functions. The donor states thus have a degeneracy arising from the multivalley nature of the conduction band. The envelope wave functions satisfy the effective-mass wave equation in which the anisotropic effective mass and the dielectric constant are incorporated. Provided the dielectric constant and the effective masses char-

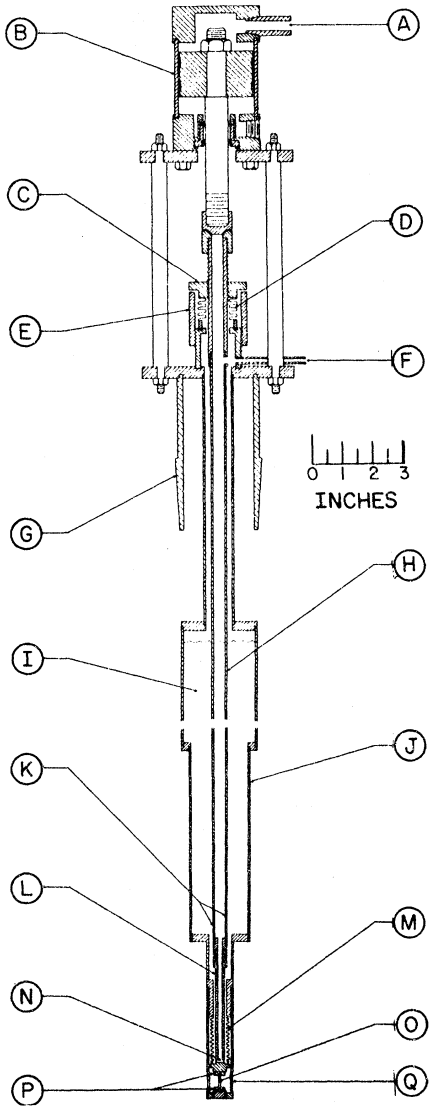

FIG. 2. Stainless-steel-stress centerpiece. This replaces the glass centerpiece shown in Fig. 1.

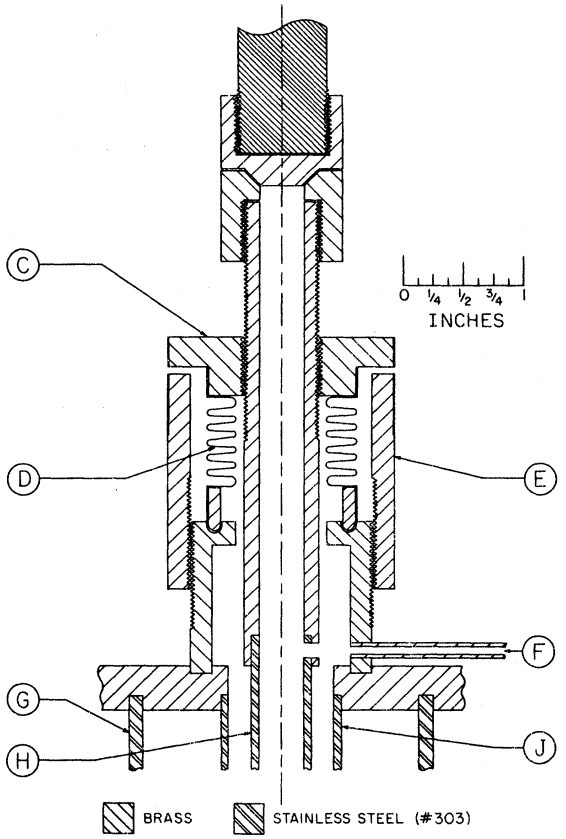

FIG. 3. Details of the upper section of the stress centerpiece.

acterizing the conduction-band minima are unaltered by a small strain, then, for given valley, the energy-level scheme of a donor will be unaffected by the stress. However, the energy-level schemes bearing different valley labels will be shifted relative to one another by the amounts given in Eq. (1). This will be true for all states which are well described by the effective-mass Hamiltonian, such as the p states. The symmetry of the donor levels must conform to the site symmetry of the donor, which is T_d in the absence of stress for the donors discussed in this paper; hence the donor wave functions will form basis functions for representations of T_d in the absence of stress and the appropriate new site symmetries when the stress is applied.[1] It is well known[2] that even for the unstressed crystal, the degeneracy of the $1s$ ground state is lifted, consistent with the T_d site symmetry, by the chemical splitting. For silicon, the totally symmetric $1s(A_1)$ level is depressed below the effective-mass position whereas the $1s(E)$ and $1s(T_2)$ levels remain close to it. Price[3] has considered the effect of strain for donors in germanium explicitly taking into account the chemical splitting; following Price, similar calculations have been made by Wilson and Feher[7] for silicon.

For the jth valley of Si, replacing $K_\alpha^{(j)}$ and $K_\beta^{(j)}$ by the direction cosines l, m, or n, we have from Eq. (1) the energy shift of the jth valley;

$$\Delta E^{(j)} = \Xi_d(u_{xx}+u_{yy}+u_{zz}) + \Xi_u(l^2u_{xx}+m^2u_{yy}+n^2u_{zz} + 2mnu_{yz} + 2nlu_{xz} + 2lmu_{xy}). \quad (2)$$

The shift of the center of gravity of the valleys will be given by

$$\langle \Delta E^{(j)} \rangle = (\Xi_d + \tfrac{1}{3}\Xi_u)(u_{xx}+u_{yy}+u_{zz}) . \quad (3)$$

The shift of a given valley with respect to the center of gravity $\delta E^{(j)}$ is

$$\delta E^{(j)} = \Xi_u(l^2u_{xx}+m^2u_{yy}+n^2u_{zz}+2mnu_{yz}+2nlu_{zx} + 2lmu_{xy}) - \tfrac{1}{3}\Xi_u(u_{xx}+u_{yy}+u_{zz}) . \quad (4)$$

The strain components $u_{\alpha\beta}$ are related to the stress components σ_{ij} by the elastic compliance constants for cubic crystals as follows[24]:

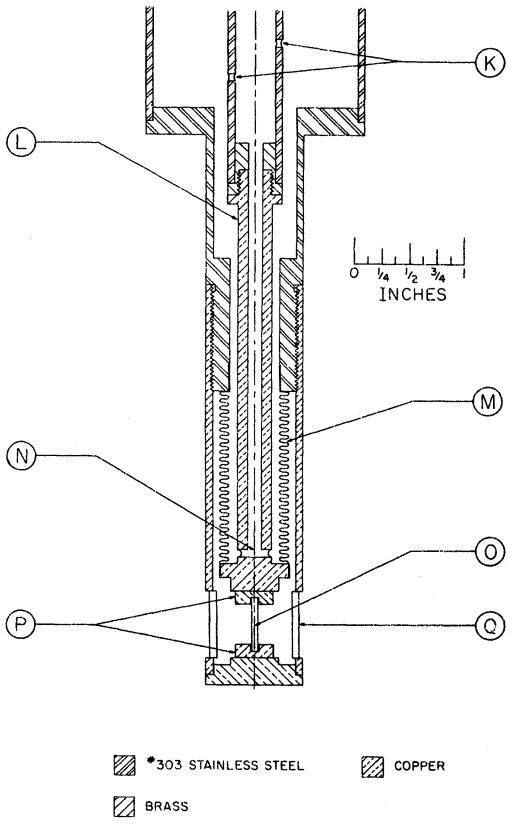

FIG. 4. Details of the lower section of the stress centerpiece.

$$\begin{bmatrix} u_{xx} \\ u_{yy} \\ u_{zz} \\ u_{yz} \\ u_{zx} \\ u_{xy} \end{bmatrix} = \begin{bmatrix} s_{11} & s_{12} & s_{12} & 0 & 0 & 0 \\ s_{12} & s_{11} & s_{12} & 0 & 0 & 0 \\ s_{12} & s_{12} & s_{11} & 0 & 0 & 0 \\ 0 & 0 & 0 & \frac{1}{2}s_{44} & 0 & 0 \\ 0 & 0 & 0 & 0 & \frac{1}{2}s_{44} & 0 \\ 0 & 0 & 0 & 0 & 0 & \frac{1}{2}s_{44} \end{bmatrix} \begin{bmatrix} \sigma_{xx} \\ \sigma_{yy} \\ \sigma_{zz} \\ \sigma_{yz} \\ \sigma_{zx} \\ \sigma_{xy} \end{bmatrix} . \tag{5}$$

Thus,

$$\delta E^{(j)} = \Xi_u \{(s_{11} - s_{12})[l^2\sigma_{xx} + m^2\sigma_{yy} + n^2\sigma_{zz} - \tfrac{1}{3}(\sigma_{xx} + \sigma_{yy} + \sigma_{zz})] + s_{44}(mn\sigma_{yz} + ln\sigma_{zx} + lm\sigma_{xy})\} . \tag{6}$$

Compact expressions for $\delta E^{(j)}$ can be obtained in the following manner: Let $\hat{F}$ be a unit vector along the direction of the applied force $\vec{F}$ then

$$\sigma_{pq} = \pm (\hat{F} \cdot \hat{p})(\hat{F} \cdot \hat{q}) T, \quad p, q = x, y, z \tag{7}$$

where the positive sign is used for tension and the negative sign for compression, and T is the magnitude of $\vec{F}$ divided by the cross-sectional area of the sample. Also let $\hat{R}_j$ be a unit vector along the direction from the center of the Brillouin zone to the jth valley. Then for silicon with the six valleys 1, . . . , 6 along [100], [$\bar{1}$00], [010], [0$\bar{1}$0], [001], and [00$\bar{1}$], respectively, as shown in Fig. 6, Eq. (6) for compressive force reduces to

$$\delta E^{(j)} = -\Xi_u T (s_{11} - s_{12})[(\hat{R}_j \cdot \hat{F})^2 - \tfrac{1}{3}] . \tag{8}$$

For a general direction of force $\vec{F}$ with θ and ϕ as defined in Fig. 6, one obtains

$$\begin{aligned} \delta E^{(1,2)} &= -T\Xi_u(s_{11} - s_{12})(\cos^2\theta \sin^2\phi - \tfrac{1}{3}) , \\ \delta E^{(3,4)} &= -T\Xi_u(s_{11} - s_{12})(\sin^2\theta \sin^2\phi - \tfrac{1}{3}) , \\ \delta E^{(5,6)} &= -T\Xi_u(s_{11} - s_{12})(\cos^2\phi - \tfrac{1}{3}) . \end{aligned} \tag{9}$$

Figure 7 depicts $\delta E^{(j)}$ as a function of θ and ϕ for a given compressive force as given by Eqs. (9). It is clear from the figure that for an arbitrary direction of applied force each excited state will, in general, split into three sublevels. The following features corresponding to the force applied along directions of high symmetry should be noted: For $\vec{F} \parallel [111]$, i.e., $\theta = 45°$ and $\phi = \arccos(1/\sqrt{3})$, $\delta E^{(j)} = 0$ for all j; for $\vec{F} \parallel [100]$, i.e., $\theta = 0°$, $\phi = 90°$, $\delta E^{(1,2)} = -\frac{2}{3} T\Xi_u(s_{11} - s_{12})$, and $\delta E^{(3,4)} = \delta E^{(5,6)} = \frac{1}{3} T\Xi_u(s_{11} - s_{12})$ and the excited states split into two sublevels, the one of lower energy being shifted

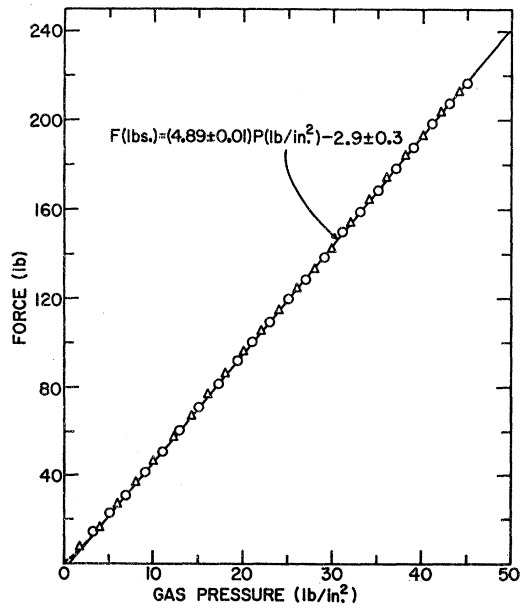

FIG. 5. Calibration of the pressure head, i.e., resultant force vs applied gas pressure. The solid line represents a least-squares fit to four sets of data points, two of which are shown in the figure; P is the gas pressure. These were obtained in the direction of increasing pressure. Note the nonlinear section below ~5 lb/in.^{2} of gas pressure.

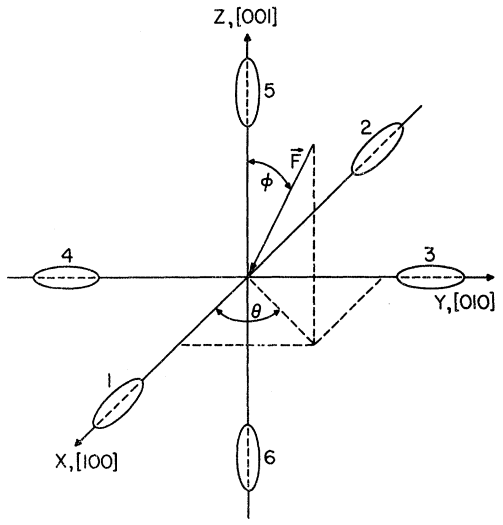

FIG. 6. Constant energy ellipsoids of the conduction-band minima of silicon along ⟨100⟩. Also shown, for convenience, are the coordinate axes, the direction of applied compressive force $\vec{F}$, and its polar coordinates.

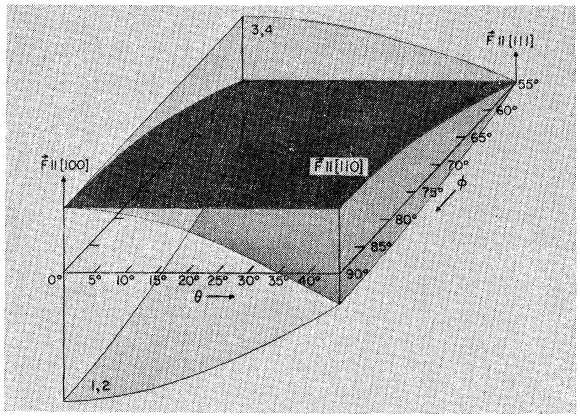

FIG. 7. Energy shifts of the conduction-band valleys of silicon from the center of gravity as a function of θ and ϕ, defined in Fig. 6, for a given compressive force. The horizontal plane corresponds to the center of gravity of the valleys. The energy sheet labeled "1,2" corresponds to valleys along [100] and [$\bar{1}$00], the sheet labeled "3,4" corresponds to valleys along [010] and [0$\bar{1}$0], and the third sheet corresponds to valleys along [001] and [00$\bar{1}$].

twice as much below the center of gravity as the other is shifted above it; for $\vec{F} \parallel [110]$, i.e., $\theta = 45°$, $\phi = 90°$, $\delta E^{(1,2)} = \delta E^{(3,4)} = -\frac{1}{6} T\Xi_u(s_{11} - s_{12})$ and $\delta E^{(5,6)} = \frac{1}{3} T\Xi_u(s_{11} - s_{12})$, and again the excited states are split into two substates but now the higher-energy sublevel is the one which is shifted twice as much above the center of gravity. It is interesting to note that for $\phi = \arccos(1/\sqrt{3})$ and θ arbitrary, the excited states are split into three sublevels, one remaining at the center of gravity and the other two symmetrically displaced about it. This is also true for $\phi = 90°$ and $\theta = \arccos\sqrt{\frac{2}{3}}$. It can also be seen from the figure that a much smaller misalignment of the force from the desired direction is required to produce a third sublevel for $\vec{F} \parallel [110]$ as compared to $\vec{F} \parallel [100]$.

In addition to the chemical splitting, the energy of the ground states vary as a function of stress. A calculation by Wilson and Feher,[7] for silicon with $\vec{F} \parallel [100]$ yields the following result for the shift of the singlet $1s(A_1)$ ground state from its zero-stress position;

$$\delta E_{gs} = \Delta_c[3 + \tfrac{1}{2}x - \tfrac{3}{2}(x^2 + \tfrac{4}{3}x + 4)^{1/2}], \qquad (10)$$

where $6\Delta_c$ is the singlet-doublet splitting of the ground state and

$$x = -[\Xi_u(s_{11} - s_{12})T]/3\Delta_c$$

for compression.

IV. EXPERIMENTAL RESULTS AND DISCUSSION

Figure 8 shows a typical spectrum of arsenic donors in silicon under a uniaxial compression of 3.7×10^8 dyn/cm^2. The lines observed are those

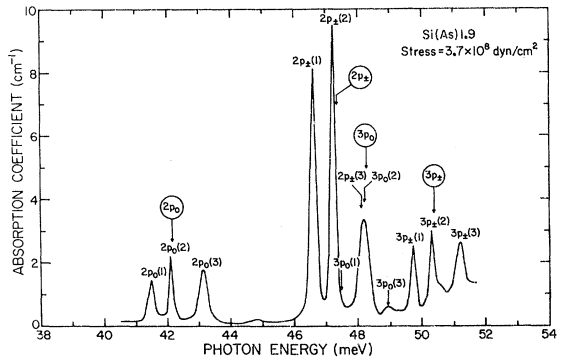

FIG. 8. $1s(A_1) \rightarrow 2p_0$, $2p_\pm$, $3p_0$, and $3p_\pm$ lines of the excitation spectrum of arsenic-doped silicon under compressive force along a direction with $\theta = 39.3°$ and $\phi = 74.6°$ (see text). Liquid helium used as coolant. The zero-stress positions are indicated with arrows. Room-temperature resistivity $\sim 6\ \Omega$ cm.

corresponding to $1s(A_1) \rightarrow np$ transitions. In this case, the force was applied along a direction close to $\theta = 36.2°$ and $\phi = 77.8°$. As can be seen, each excitation line is split into three components with the central component very near the zero-stress position. Had the force been precisely along the

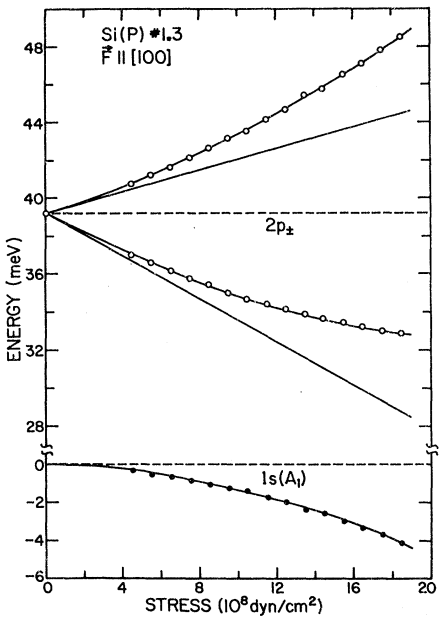

FIG. 9. Stress dependence of the energies of the two components of the $1s(A_1) \rightarrow 2p_\pm$ line of phosphorus donors in silicon for $\vec{F} \parallel [100]$. Liquid helium used as coolant. The solid straight lines are the energy shifts of the two components of the $2p_\pm$ line from the zero-stress position, calculated from their energy difference divided in the ratio of 2:1. The curved solid line represents the shift of the $1s(A_1)$ state with stress; the solid points were computed by taking the difference between the straight line and the data points.

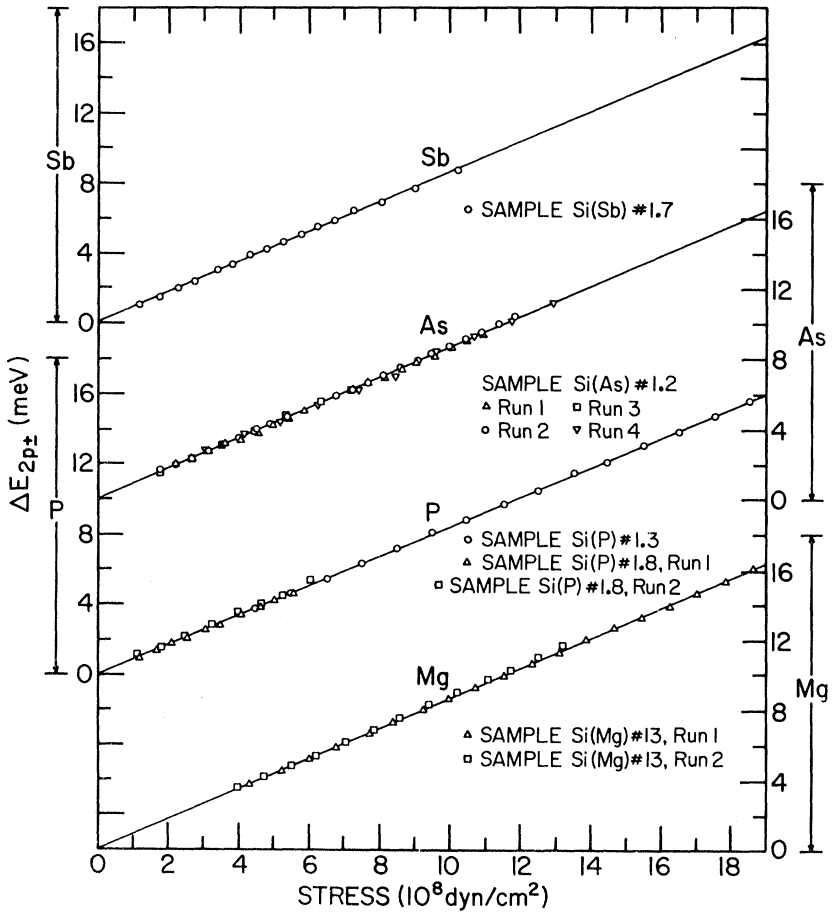

FIG. 10. Splitting of the $2p_{\pm}$ line with $\vec{F} \parallel [100]$ as a function of stress for Sb, As, P, and Mg donors in silicon. The solid lines represent least-squares fit to all the data for a given impurity. The slope m of each line is $m(\mathrm{Sb}) = 0.853 \pm 0.001$; $m(\mathrm{As}) = 0.860 \pm 0.002$; $m(\mathrm{P}) = 0.844 \pm 0.002$; $m(\mathrm{Mg}) = 0.853 \pm 0.003$. Room-temperature resistivity: Si(Sb) ~ 15 Ω cm; Si(As) ~6 Ω cm; Si(P) # 1.3 ~6 Ω cm; Si(P) # 1.8 ~6 Ω cm; Si(Mg) estimated to be ~5 Ω cm.

direction corresponding to the values of θ and ϕ given above, the central component would have remained at the zero-stress position and the other two components would have been equally displaced on either side of it. From the observed splittings, using Eqs. 9 and a value of $\Xi_u = 8.77$ eV (see later), θ and ϕ were calculated to be 39.3° and 74.6°, respectively; these values were found to be consistent with an x-ray orientation of the sample. Observations were also made for $\vec{F} \parallel [100]$ and [110]. As mentioned earlier, for the latter orientation the alignment of the applied force is very critical. In most of the measurements made for this orientation, the lower-energy component was observed to split into two. This observation could be accounted for by assuming misorientations of about 2°. Hence measurements from which Ξ_u was deduced were confined to $\vec{F} \parallel [100]$. In the present investigation, polarized radiation was not used; a detailed study of the polarization effects and selection rules has been described in an earlier publication.[25]

In Fig. 9 are shown the positions of the high- and low-energy components of the $2p_{\pm}$ line as a function of stress for phosphorus donors in silicon with $\vec{F} \parallel [100]$. The difference in energy between the two components is given by

$$\Delta E_{2p_{\pm}} = \delta E^{(3,4,5,6)} - \delta E^{(1,2)} = T\Xi_u(s_{11} - s_{12}). \quad (11)$$

Thus a plot of $\Delta E_{2p_{\pm}}$ vs T will lead to a direct determination of Ξ_u. Figure 10 shows such a plot for the four impurities studied in the present investigation. The solid lines represent the least-squares fit to the data points. With $s_{11} - s_{12} = (9.745 \pm 0.02\%) \times 10^{-13}$ cm^2/dyn at 4.2 °K for silicon,[26] the values of the shear-deformation-potential constant obtained are[27]

$$\Xi_u(\mathrm{Sb}) = 8.76 \pm 0.13 \text{ eV}, \quad \Xi_u(\mathrm{As}) = 8.76 \pm 0.25 \text{ eV},$$

$$\Xi_u(\mathrm{P}) = 8.65 \pm 0.20 \text{ eV}, \quad \Xi_u(\mathrm{Mg}) = 8.91 \pm 0.20 \text{ eV};$$

the errors indicated were obtained by adding the fractional errors in the determination of the cross-sectional area, in the calibration of force vs pressure (Fig. 5), and in the slopes of $\Delta E_{2p_{\pm}}$ vs stress. The values of Ξ_u were computed for each individual run and the above values represent an average. Thus the present investigation demonstrates that within experimental error, Ξ_u is the same for all impurities with an average value of $\Xi_u = 8.77 \pm 0.07$

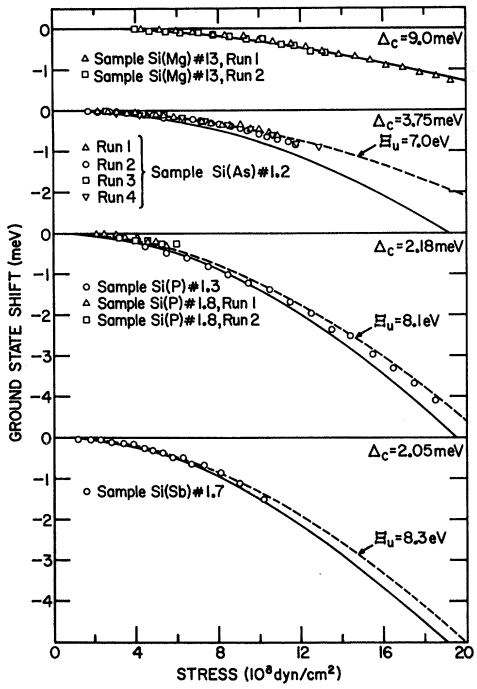

FIG. 11. The shift of the $1s(A_1)$ ground state as a function of stress, deduced in the manner shown in Fig. 9. The solid line for each impurity is calculated using the value of Δ_c shown and $\Xi_u = 8.77$ eV in Eq. (10). The dotted curves for Sb, P, and As were obtained with the values of Ξ_u and Δ_c shown for each impurity; the values of Ξ_u were obtained from Fig. 12.

eV, where the mean absolute error is given. In the spirit of the effective-mass theory, this value should thus represent the shear-deformation-potential constant of the conduction-band minima of silicon and is included in Table I.

Also shown in Fig. 9 with solid lines are the energy shifts of the two components of the $2p_{\pm}$ line from the zero-stress position calculated from their energy difference divided in the ratio of 2:1, predicted theoretically. If one assumes that the difference between the solid straight lines and the actual data is solely due to the shift of the $1s(A_1)$ ground state, then this shift can be determined and is shown by the curve at the bottom of the figure. The shift of the $1s(A_1)$ ground state as a function of stress, calculated in this manner for all the impurities studied in the present investigation, is shown in Fig. 11. Also shown, as solid lines, are the shifts calculated using Eq. (10) and the experimentally determined values of $6\Delta_c$ and Ξ_u, viz., $6\Delta_c = 12.28$, 13.10, and 22.5 meV for antimony, phosphorus, and arsenic,[28] respectively, and $\Xi_u = 8.77$ eV. In the case of magnesium,[27] $6\Delta_c$ is not known experimentally. The solid curve in Fig. 11 for magnesium is drawn for $\Xi_u = 8.77$ eV and $6\Delta_c = 54$ meV; a value of 55 ± 3 meV is obtained by averaging the results of $6\Delta_c$ computed from Eq. (10) for each data point. As can be seen, the solid curves for the group-V impurities depart from the data, the discrepancy being most significant for arsenic and least for antimony. Following Wilson and Feher,[7] x as a function of $s' = -2(s_{11} - s_{12})T$ can be obtained from Eq. (10) by using the experimentally determined values of δE_{ss}, and Δ_c. Figure 12 shows this dependence and the least-squares fits, assuming a linear dependence of x on s'. From the slopes of the lines the values of Ξ_u obtained are 8.3, 8.1, and 7.0 eV, for antimony, phosphorous, and arsenic, respectively. The dashed curves in Fig. 11 are drawn for these values of Ξ_u. Interpreted in this fashion, the shear-deformation-potential constant deduced from the ground-state shift appears to be dependent on the chemical species of the donor.

V. CONCLUDING DISCUSSION

As pointed out in Sec. I, it is evident from Table I that the measured values of Ξ_u fall into two groups, viz., one clustered about 8.5 eV and the other about 11 eV. It is interesting to note that, except for the piezo-optic measurement of Schmidt-

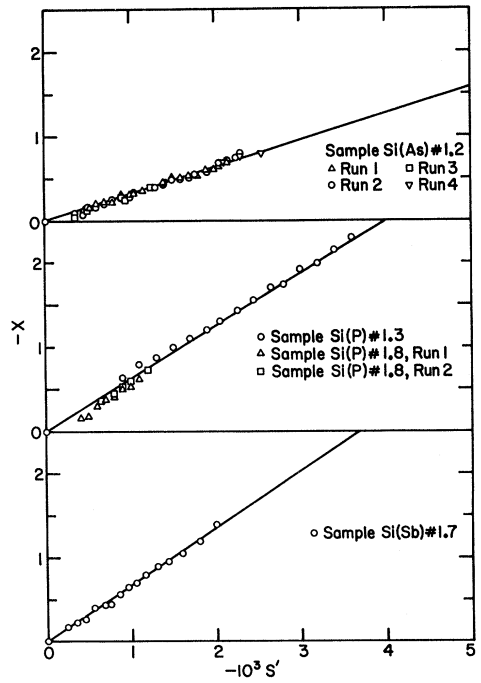

FIG. 12. Plot of $x = [-\Xi_u(s_{11} - s_{12})T]/3\Delta_c$ vs $s' = -2(s_{11} - s_{12})T$ for compression. The values for x were obtained using Eq. (10) together with the appropriate experimentally determined values for Δ_c (Ref. 28). The solid straight lines represent least-squares fit to the calculated points. The values of Ξ_u determined from the slopes of the straight lines are $\Xi_u(\mathrm{Sb}) = 8.3$ eV, $\Xi_u(\mathrm{P}) = 8.1$ eV, and $\Xi_u(\mathrm{As}) = 7.0$ eV.

Tiedemann,[29] all those techniques which directly measured the effect of stress on the conduction-band minima yielded values in the lower group. It is gratifying that the values of Ξ_u determined in the present investigation and those of Krag *et al.*,[5,6] from the piezospectroscopy of the *excited states*, fall in the lower group. It is evident from the table that the spread in the values of Ξ_u cannot be attributed to any significant temperature dependence of this quantity.

Two of the measurements which give values in the higher group utilize the effect of uniaxial stress on the EPR of the donor electron in the $1s(A_1)$ ground state. The discrepancy between the two groups of values has been pointed out previously,[8,28] and has yet to be explained. The situation has become even more intriguing in that the values of Ξ_u deduced in the present investigation for $1s(A_1)$ states are *lower* than those obtained for the excited states and further, seem to depend on the chemical nature of the donor. Krag *et al.*[6] have also obtained a smaller value of Ξ_u from the stress dependence of the ground states of bismuth donors in silicon. Castner *et al.*[30] have considered corrections to the $1s(A_1)$ wave function based on the $\langle 100 \rangle$ minima by admixing the low-energy regions of the lowest conduction band and have proposed that as a consequence the shear-deformation-potential constant of this state is donor dependent and need not be the same as that of the conduction-band edge.

ACKNOWLEDGMENTS

The authors wish to thank Professor S. Rodriguez for several useful discussions and Professor H. J. Yearian and Miss L. Roth for crystal orientation. They also thank Dr. A. Onton and Dr. W. E. Krag for information regarding their stress cryostats. Special thanks are due to J. B. Moore and H. E. Larson for suggestions in the design and for the construction of the stress centerpiece.

---

*Work supported by the National Science Foundation and the Advanced Research Projects Agency.

†Honeywell Fellow (1970–1972).

[1]P. Fisher and A. K. Ramdas, *Physics of the Solid State*, edited by S. Balakrishna, M. Krishnamurthi, and B. Ramachandra Rao (Academic, New York, 1969), p. 149.

[2]W. Kohn, *Solid State Physics*, edited by F. Seitz and D. Turnbull (Academic, New York, 1957), Vol. 5, p. 257.

[3]P. J. Price, Phys. Rev. 104, 1223 (1956).

[4]G. L. Bir, E. I. Butikov, and G. E. Pikus, J. Phys. Chem. Solids 24, 1467 (1963).

[5]W. E. Krag, W. H. Kleiner, H. J. Zeiger, and S. Fischler, J. Phys. Soc. Japan Suppl. 21, 230 (1966).

[6]W. E. Krag, W. H. Kleiner, and H. J. Zeiger, in *Proceedings of the Tenth International Conference on the Physics of Semiconductors, Cambridge, Mass.*, 1970, edited by S. P. Keller, J. C. Hensel, and F. Stern (U. S. Atomic Energy Commission, Division of Technical Information, Washington, D. C., 1970), p. 271.

[7]D. K. Wilson and G. Feher, Phys. Rev. 124, 1068 (1961).

[8]G. D. Watkins and F. S. Ham, Phys. Rev. B 1, 4071 (1970).

[9]R. L. Aggarwal, Ph. D. thesis (Purdue University, 1965) (unpublished).

[10]P. Fisher, W. H. Haak, E. J. Johnson, and A. K. Ramdas, in *Proceedings of the Eighth Symposium on the Art of Glass Blowing* (The American Scientific Glass Blowers Society, Wilmington, Del., 1963), p. 136.

[11]Kontes of Illinois, 1916 Greenleaf Avenue, Evanston, Ill.

[12]Model No. D-49, Alkon Products Corp., 25 Power Avenue, Wayne, N. J. 07470.

[13]V. J. Tekippe and A. K. Ramdas, Phys. Letters 35A, 143 (1971).

[14]Servometer Corp., 82 Industrial East, Clifton, N. J.

[15]Model No. 63115, Precision Scientific Co., 3737 W. Cortiand St., Chicago 47, Ill.

[16]Matheson Gas Products, P. O. Box 96, Joliet, Ill. 60434.

[17]Model No. 410-RTD (Accuracy $\frac{1}{4}$ of 1%), Booth/Spearing, 5335 W. Raymond, Indianapolis, Ind. 46241.

[18]We wish to thank the Department of Civil Engineering, Purdue University, especially W. B. Telfer, for the use of their tensile-stress apparatus.

[19]Model No. 34-0862 AY, Toledo Scale Co., 5225 Telegraph Rd., Toledo, Ohio 43612.

[20]R. D. Hancock and S. Edelman, Rev. Sci. Instr. 27, 1082 (1956).

[21]A. Smakula and V. Sils, Phys. Rev. 99, 1744 (1955).

[22]GE-7031 Varnish, Insulating Materials Department, General Electric Co., Schenectady, N. Y.

[23]C. Herring, Bell System Tech. J. 34, 237 (1955); C. Herring and E. Vogt, Phys. Rev. 101, 944 (1956).

[24]J. F. Nye, *Physical Properties of Crystals* (Oxford U. P., Oxford, London, 1964).

[25]R. L. Aggarwal and A. K. Ramdas, Phys. Rev. 137, A602 (1965).

[26]J. J. Hall, Phys. Rev. 161, 756 (1967). It is estimated from the data in this paper that the value of $(s_{11} - s_{12}) \sim 10\,^{\circ}\mathrm{K}$, the temperature at which our measurements were made, does not differ significantly from that at 4.2 °K.

[27]L. T. Ho and A. K. Ramdas, Phys. Rev. B 5, 462 (1972).

[28]R. L. Aggarwal and A. K. Ramdas, Phys. Rev. 140, A1246 (1965).

[29]K. J. Schmidt-Tiedemann, in *Proceedings of the International Conference on the Physics of Semiconductors, Exeter* 1962 (The Institute of Physics and the Physical Society, London, 1962), p. 191.

[30]T. G. Castner, Jr., E. B. Hale, and R. Craven, Ref. 6, p. 613; T. G. Castner, Jr., Phys. Rev. B 2, 4911 (1970).

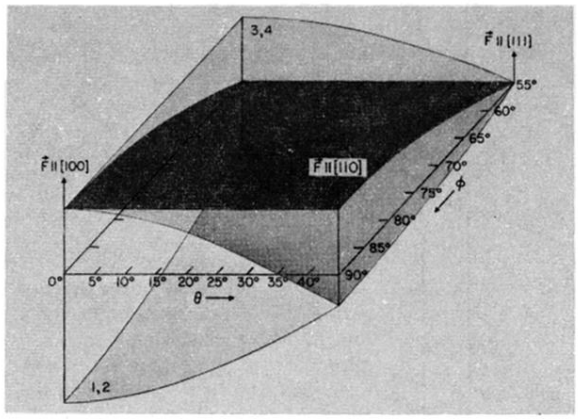

FIG. 7. Energy shifts of the conduction-band valleys of silicon from the center of gravity as a function of θ and ϕ, defined in Fig. 6, for a given compressive force. The horizontal plane corresponds to the center of gravity of the valleys. The energy sheet labeled "1, 2" corresponds to valleys along [100] and [$\bar{1}$00], the sheet labeled "3, 4" corresponds to valleys along [010] and [0$\bar{1}$0], and the third sheet corresponds to valleys along [001] and [00$\bar{1}$].